JACS
JOURNAL OF THE AMERICAN CHEMICAL SOCIETY

Article

pubs.acs.org/JACS

Probing Dynamic Conformations of the High-Molecular-Weight αB-Crystallin Heat Shock Protein Ensemble by NMR Spectroscopy

Andrew J. Baldwin,*[,†,‡] Patrick Walsh,[‡,§] D. Flemming Hansen,[†,∥] Gillian R. Hilton,[⊥] Justin L. P. Benesch,[⊥] Simon Sharpe,[‡,§] and Lewis E. Kay*[,†,‡,§]

[†]Departments of Molecular Genetics and Chemistry, The University of Toronto, Toronto, Ontario M5S 1A8, Canada

[‡]Department of Biochemistry, The University of Toronto, Toronto, Ontario M5S 1A8, Canada

[§]Program in Molecular Structure, Hospital for Sick Children, 555 University Avenue, Toronto, Ontario M5G 1X8, Canada

[⊥]Physical and Theoretical Chemistry Laboratory, Department of Chemistry, University of Oxford, South Parks Road, Oxford, Oxfordshire OX1 3QZ, U.K.

Supporting Information

ABSTRACT: Solution- and solid-state nuclear magnetic resonance (NMR) spectroscopy are highly complementary techniques for studying supra-molecular structure. Here they are employed for investigating the molecular chaperone αB-crystallin, a polydisperse ensemble of between 10 and 40 identical subunits with an average molecular mass of approximately 600 kDa. An IxI motif in the C-terminal region of each of the subunits is thought to play a critical role in regulating the size distribution of oligomers and in controlling the kinetics of subunit exchange between them. Previously published solid-state NMR and X-ray results are consistent with a bound IxI conformation, while solution NMR studies provide strong support for a highly dynamic state. Here we demonstrate through FROSTY (*f*reezing *r*otational diffusion *o*f protein *s*olutions at low *t*emperature and high viscosit*y*) MAS (*m*agic *a*ngle *s*pinning) NMR that both populations are present at low temperatures (<0 °C), while at higher temperatures only the mobile state is observed. Solution NMR relaxation dispersion experiments performed under physiologically relevant conditions establish that the motif interchanges between flexible (highly populated) and bound (sparsely populated) states. This work emphasizes the importance of using multiple methods in studies of supra-molecules, especially for highly dynamic ensembles where sample conditions can potentially affect the conformational properties observed.

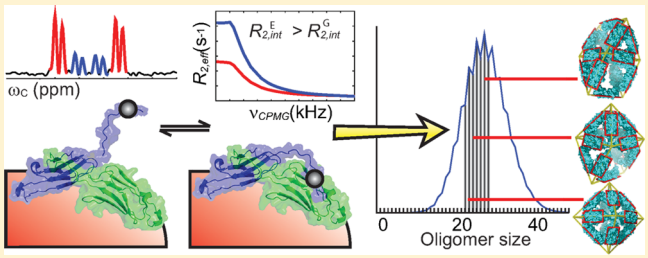

INTRODUCTION

The native states of proteins are in many cases inherently unstable,[1] and the assistance of "molecular chaperones" is required to ensure that these important biomolecules attain and maintain their functional forms.[2,3] The molecular chaperone αB-crystallin is a human small heat shock protein (sHSP) that plays an important role in proteostasis *in vivo*[4,5] and can prevent amyloid fibril formation *in vitro*.[6] It is up-regulated in neuronal cells of patients suffering from neurodegenerative disorders including Alzheimer's and Parkinson's diseases, where it is found bound to amyloid plaques.[7] An understanding of how this chaperone inhibits protein aggregation has proven elusive. Structural studies are challenged by the fact that αB-crystallin populates a heterogeneous ensemble of inter-converting oligomers at equilibrium, with 95% of the oligomers sized between 20- and 40-mers.[8] Despite this complexity, αB-crystallin oligomers possess several remarkably simplifying features. Both solid- and solution-state nuclear magnetic resonance (NMR) studies have established that the overall structure adopted by the constituent monomers is essentially independent of oligomer size.[9,10] In addition, we have previously shown that the equilibrium size distribution can be quantitatively explained assuming that both the dimer interface and the interface holding neighboring dimers together are similar in all oligomers.[8] These observations have allowed us to construct structural models of the principally populated oligomers in solution (Figure 1A).[11] Alternative models of αB-crystallin have also been recently put forward.[12,13]

The primary sequence of αB-crystallin and of sHSPs in general can be divided into three parts,[14−16] the N- and C-termini and a core domain (Figure 1A-i). The termini are involved in holding the oligomers together, and the motional properties of a highly conserved IxI motif in the C-terminus are thought to play a critical role in regulating the kinetics and thermodynamics of monomer exchange between oligomers.[9] The end of the C-terminus, a region termed the "extension" (green in Figure 1A-i), is intrinsically disordered. For example, residues 164−175 were observed in solution ^{1}H NMR spectra using experiments and samples that were not optimized for

Received: April 20, 2012
Published: August 23, 2012

   dx.doi.org/10.1021/ja307874r | J. Am. Chem. Soc. 2012, 134, 15343−15350

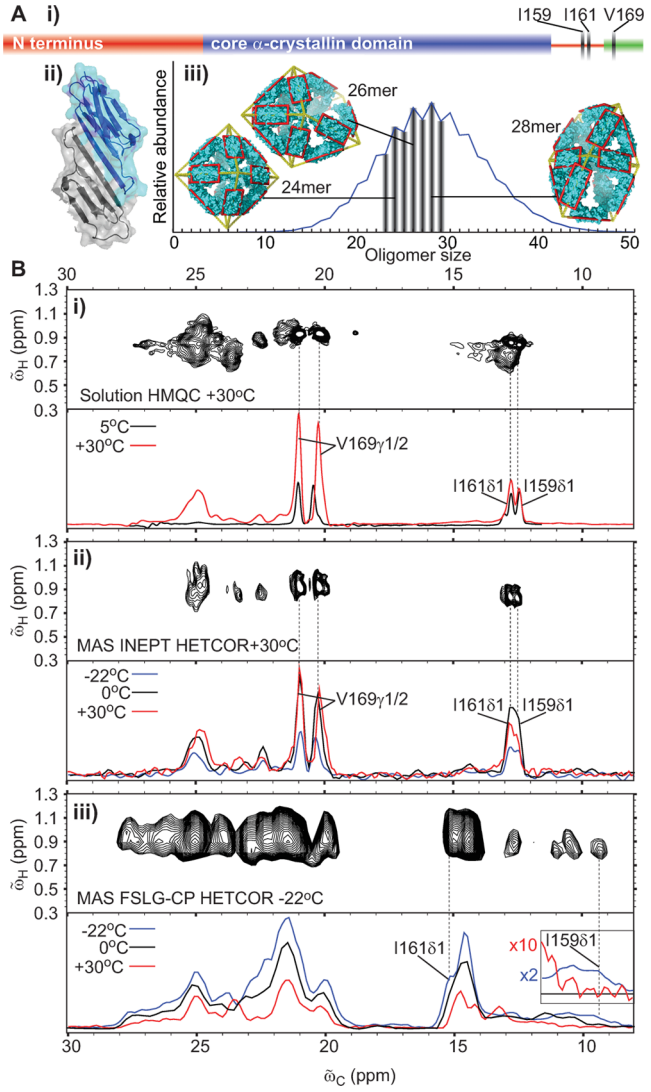

Figure 1. (A) (i) The sequence of αB-crystallin can be separated into three regions, an N-terminus (1−57), the core α-crystallin domain, and the C-terminus (149−175). (ii) The core domain adopts a β-sheet-rich fold which dimerizes. The basic building block dimeric structure of αB-crystallin, lacking the N and C termini, is illustrated (PDB accession code 2wj7[25]). (iii) The core dimer structure assembles into a wide range of inter-converting oligomers in solution.[8] Structural models of the 23- to 29-mers (bars) have recently been determined.[11] (B) (i) Solution NMR spectrum of U-[^{2}H], Ile-[$^{13}CH_3$ δ1], Leu,Val-[$^{13}CH_3$,$^{12}CD_3$] αB-crystallin, 30 °C, 14.0 T, pH 7, with prominent resonances from the C-terminal methyl groups of I159δ1, 161δ1, and V169γ1/γ2. Correlations for all nine isoleucine residues in αB-crystallin are observed in spectra recorded on samples with only Ile labeling,[9] with only a single resonance obtained for each Iδ1. The upfield correlation observed for I159δ1 in the cross-polarization magic angle spinning (CP-MAS) spectrum, −22 °C, at 9.5 ppm (see iii) is shifted to 12.3 ppm in solution; a peak is not observed at 9.5 ppm. (ii) FROSTY-MAS[33] spectrum of U-[^{2}H], Ile-[$^{13}CH_3$ δ1], Leu,Val-[$^{13}CH_3$,$^{12}CD_3$] αB-crystallin, 30 °C, 11.7 T, pH 7, with ^{1}H-to-^{13}C polarization transfer achieved via INEPT.[52] This spectrum is very similar to the solution data set. (iii) As in (ii) but with polarization transfer via CP,[51] −22 °C, 11.7 T. Notably, resonances from I159δ1 and I161δ1 at $\tilde{\omega}_C$ values of 9.5 and 15 ppm, respectively, can be clearly discerned. At temperatures of 0 °C and higher, this resonance for I159δ1 is no longer observed. While the intensity of the peak derived from I161δ1 appears to decrease with temperature as well, this is difficult to conclude with certainty because of the appreciable overlap in this region.

large proteins, which is only possible if this region is highly mobile.[17−19] Of interest, mutations in the C-terminus modulate chaperone activity[20,21] and have been linked to disease.[22−24]

When both of the termini are removed, the core domain forms β-sheet-rich dimers (Figure 1A-ii) that serve as the "building blocks" for the oligomeric structures.[25,26] Deletion of the N terminus and the C-terminus past the IxI motif (residues 159−161 in αB-crystallin, Figure 1A-i) leads to predominantly monomers and dimers in solution, although a significant population of oligomers remains.[27] When crystallized, the IxI residues in this deletion construct form contacts between dimers,[27] mimicking an interaction observed in crystal structures of homologous sHSP oligomers.[28,29] Notably, solid-state NMR studies of αB-crystallin comprising full-length protein establish that each dimeric unit adopts a structure similar to that in Figure 1A-ii, with the IxI residues tightly bound to adjacent dimers.[10] In contrast, a different picture has emerged from solution-state NMR, where spin relaxation studies of the IxI residues show that they are highly mobile.[9] Indeed, the ^{13}C chemical shifts of the Ile δ1 carbons in the IxI motif, 12.5 and 12.3 ppm, are consistent with the values observed for a random coil.[30] Although it is clear that in solution the IxI motif is disordered and unbound, paramagnetic relaxation enhancement NMR measurements establish that these residues, nevertheless, are localized to a region proximal to a binding pocket[9] that has been elucidated by solid-state NMR and X-ray diffraction studies[10,27]

In order to resolve this apparent discrepancy and to further characterize the dynamics of the IxI residues, we have employed a combination of both solution- and solid-state NMR using U-[^{2}H], Ile-[$^{13}CH_3$ δ1], Leu,Val-[$^{13}CH_3$,$^{12}CD_3$] samples of αB-crystallin. The solution NMR experiments exploit a methyl-TROSY effect that is critical in studies of very high molecular weight proteins (average molecular mass of 580 kDa).[31,32] Following the elegant work of Reif, Oshkinat, and co-workers on the αB-crystallin system[33] we have used MAS NMR of samples sedimented by ultracentrifugation[34] and prepared according to the FROSTY protocol (referred to as FROSTY-MAS below) to examine both the "liquid-like" and "solid-like" properties of the IxI motif of αB-crystallin. By using the same sample labeling for both sets of experiments, the solution- and solid-state NMR results can be compared directly. Moreover, the extensive protein deuteration that benefits the solution NMR studies is also advantageous in removing unwanted dipolar interactions in the solid-state-based experiments. We show here, through a combination of both solution- and solid-state NMR techniques, that at temperatures below 0 °C the IxI moiety exists in at least two states, corresponding to bound and highly mobile conformations, while above 0 °C only the mobile state is observed in NMR spectra. Solution NMR relaxation dispersion (RD) studies establish further that the mobile IxI conformation interchanges with a sparsely populated state that, remarkably, has structural features that are similar to those of the bound state that has been characterized previously by both solid-state NMR[10] and X-ray diffraction.[27]

MATERIALS AND METHODS

Protein Production and Purification. αB-Crystallin was prepared by overnight expression in *E. coli* BL21(DE3) cells at 37 °C. Cells were harvested and lysed in 20 mM Tris pH 8 buffer in the presence of a protease inhibitor cocktail (Roche). After purification on a Q-column, with protein eluting at 100 mM NaCl,[35] the fractions containing αB-crystallin were pooled, concentrated, and further

dx.doi.org/10.1021/ja307874r | J. Am. Chem. Soc. 2012, 134, 15343−15350

purified using an S200 gel filtration column in 150 mM NaCl, 50 mM Tris, pH 8.0. U-^{2}H,Ile-[$^{13}CH_3$-δ1] protein was prepared by growing in D_2O and M9 media with [^{12}C,^{2}H] glucose as the sole carbon source and the precursor sodium α-ketobutyrate [$^{13}CH_3CD_2COCO_2Na$] (60 mg/L) added 1 h prior to induction.[36] U-[^{2}H], Ile-[$^{13}CH_3$ δ1], Leu,Val-[$^{13}CH_3$,$^{12}CD_3$] αB-crystallin was generated as for Ile-labeled protein, with the addition of α-ketoisovalerate [$^{13}CH_3CD_3CDCOCO_2Na$] (80 mg/L) as described previously.[36] NMR samples in the concentration range 200 μM to 1.5 mM were transferred into a buffer containing 2 mM EDTA, 2 mM NaN_3, and 30 mM sodium phosphate in 100% D_2O, adjusted to the desired pH with DCl and NaOD. Samples for solid-state NMR were then mixed with glycerol and further concentrated, as described below.

In order to obtain the assignments of I159δ1, I161δ1, and V169γ1,γ2 methyl groups, as described previously,[9] we have used a mutagenesis approach involving the production of I159V/I161V U-[^{2}H], Ile-[$^{13}CH_3$ δ1]-αB and I161A/V169S U-[^{2}H], Ile-[$^{13}CH_3$ δ1],Leu,Val-[$^{13}CH_3$,$^{12}CD_3$] αB-crystallin samples.[9] Notably, both samples expressed at levels that were comparable to that of the wild type and eluted at the same volume as wild type when purified by size exclusion chromatography. The details of the assignment are provided in Figure S1.

Solution-State NMR Measurements. ^{13}C−^{1}H correlation spectra were acquired using Varian NMR spectrometers operating at field strengths of 11.7 T (room temperature probe), 14.0 T (cryogenically cooled probe), and 18.8 T (room temperature probe) over a range of pHs (5−9) and temperatures (5−50 °C) using experiments that exploit a methyl-TROSY effect, described in detail previously.[31,32,37−39] Relaxation data were recorded on samples at pH 5 where the effects of chemical exchange are maximal. Data showing the same exchange process were obtained at pH 7, though the effects were significantly more challenging to quantify because the population of the excited state is considerably lower (Figure S3). All data were processed using the NMRPipe program.[40]

^{1}H transverse relaxation rates, with selection for the slowly relaxing methyl proton component, were measured as described previously[41] over a range of temperatures extending from 5 to 50 °C, pH 5, 14.0 T. Similarly, ^{1}H and ^{13}C single-quantum RD experiments[42] were performed over the same temperature range, pH 5, 14.0 and 18.8 T. A constant time Carr−Purcell−Meiboom−Gill (CPMG) relaxation delay of 40 ms was employed with 17 CPMG frequencies in the range 50−2000 Hz, including several repeat values for error analysis.[43] $R_{2,\mathrm{eff}}(\nu_{\mathrm{CPMG}})$ values were obtained via the relation $R_{2,\mathrm{eff}}(\nu_{\mathrm{CPMG}}) = -1/T_{\mathrm{relax}} \ln(I(\nu_{\mathrm{CPMG}})/I_0)$, where $I(\nu_{\mathrm{CPMG}})$ and I_0 are peak intensities with and without the 40 ms constant-time CPMG delay, respectively, and ν_{CPMG} is the inverse of twice the delay between successive 180° pulses. Values of exchange parameters were extracted from fits of $R_{2,\mathrm{eff}}(\nu_{\mathrm{CPMG}})$ profiles to a two-site exchange model, as described previously[44] using the in-house written program CATIA (http://abragam.med.utoronto.ca/software.html).[44,45]

Spin-state selective methyl ^{13}C RD experiments were performed at 50 °C, pH 5 following an approach described in detail previously.[45] A constant time CPMG element of 40 ms was used, along with 21 CPMG frequencies in the range 50−2000 Hz. Errors in $R_{2,\mathrm{eff}}$ were estimated on the basis of repeat ν_{CPMG} values.[43] Dispersion data were fitted to a two-site exchange process using a relaxation model that has been described.[9,45] Central to the work here is that residue-specific values for $S^2\tau_c$ are obtained, where S^2 is the square of an order parameter quantifying the amplitude of motion of the methyl rotation axis and τ_c is the correlation time for the assumed isotropic molecular tumbling. Thus, it is possible to establish the relative mobilities of corresponding methyl groups in the ground and excited states, as discussed below.

Solid-State NMR Measurements. αB-Crystallin protein samples were prepared for solid-state NMR analyses according to the "FROSTY" procedure of Mainz et al.[33] In brief, labeled αB-crystallin was concentrated in a 100 kDa ultrafiltration membrane to a volume of 36 μL. An equal volume of 40% glycerol was added once a concentration of approximately 50 mg/mL was obtained. The sample volume was then reduced by half, yielding a solution of 50 mg/mL protein in 20% v/v glycerol, in the NMR buffer described above. The sample (final volume 36 μL) was subsequently packed into a 3.2 mm thin walled MAS rotor using centrifugation.

Solid-state NMR spectra were acquired on a narrow-bore Varian VNMRS spectrometer operating at a field strength of 11.7 T. All experiments were performed using a triple-resonance T3 MAS probe operating in two-channel mode. In all cases the MAS frequency was 12 kHz, and ^{1}H decoupling during ^{13}C evolution, detection, and mixing periods was achieved with a 120 kHz ^{1}H two-pulse phase modulated (TPPM) scheme.[46] The sample temperature under MAS conditions was calibrated using the ^{207}Pb chemical shift of solid $PbNO_3$.[47] At −20 and +20 °C, respectively, 1 and 3 °C of sample heating was observed.

1D ^{13}C spectra were obtained under MAS using either INEPT (*i*nsensitive *n*uclei *e*nhanced by *p*olarization *t*ransfer) or CP transfer from ^{1}H, with each spectrum taking approximately 2 h to acquire. For CP experiments, ^{13}C and ^{1}H field strengths of approximately 50 and 62 kHz respectively were used, with contact times of 1.2−1.4 ms and a small linear ramp on the ^{13}C channel.[48] 2D ^{13}C−^{13}C correlation spectra were recorded using a finite-pulse radio frequency driven recoupling (RFDR)[49] sequence for ^{13}C recoupling, with a mixing period of 8 ms and 25 kHz ^{13}C fields during RFDR. The transmitter was centered within the aliphatic region for RFDR experiments, and 40 t_1 points (sweep width of 3770 Hz) were acquired in the indirect dimension, with a total experiment time of 25 h. 2D ^{1}H−^{13}C heteronuclear correlation (HETCOR) spectra were obtained using either CP or INEPT transfer following the t_1 (^{1}H evolution) period. ^{1}H homonuclear decoupling was employed during the t_1 period of the CP-based experiment using a frequency-switched Lee−Goldberg (FSLG) sequence[50] at a field strength of 80 kHz. A total of 64 t_1 points were acquired, with a sweep width of 9600 Hz in the indirect dimension and a total experiment time of 18 h. A scaling factor of $1/\sqrt{3}$ was applied to the ^{1}H chemical shift dimension of the FSLG-CP HETCOR, as previously described.[51]

RESULTS AND DISCUSSION

As described in the Introduction, the IxI motif in the C-terminal region of αB-crystallin, Figure 1A, plays a critical role in controlling the kinetics and thermodynamics of subunit interchange between the ensemble of oligomeric structures that this protein populates in solution[9] (see below). It is important, therefore, to reconcile the differences between solution-state NMR results establishing that the Ile residues are highly mobile and solid-state NMR data showing that the IxI motif is in a bound conformation, and hence (relatively) rigid. To this end we have recorded both solution- and solid-state NMR spectra (Figure 1B) using samples prepared with identical labeling to serve as a starting point for further analysis of the dynamics of this important region[19−24] (see below). FROSTY-MAS HETCOR experiments using cross-polarization (CP) for magnetization transfer have been recorded previously on samples of αB-crystallin at low temperatures.[10,33] We show here that a multiple-temperature analysis of such HETCOR spectra, measured with CP and INEPT magnetization transfers, and solution heteronuclear multiple quantum coherence (HMQC) data sets gives insight into how the structures observed by solid-state NMR relate to those populated in solution, which are the more physiologically relevant.

In a previous publication we noted that there are four very intense correlations in the Ile, Leu, Val ^{13}C,^{1}H solution HMQC spectrum of αB-crystallin,[9] derived from I159δ1, I161δ1, and V169γ1,γ2 methyl groups localized to the C-terminus of the protein (Figure 1B-i) (see also Figure S1). Interestingly, none of the N-terminal Ile residues (I3δ1, I5δ1, I10δ1) give rise to cross peaks of comparable intensities, suggesting that they are much less dynamic. The proton and carbon spins from each of I159δ1, I161δ1, and V169γ1,γ2 methyl groups have relaxation

rates and chemical shifts that are consistent with a disordered region.[9] The intensities of the V169γ resonances increase with temperature in a manner consistent with increased tumbling rates. In contrast, I159δ1 and I161δ1 peak intensities increase much less significantly and in fact decrease at higher temperatures, consistent with a conformational exchange process that becomes more significant with increasing temperature.[9] The observed intensity vs temperature profile for these Ile and Val residues does not reflect different temperature dependencies for ^{1}H T_1 values, as measurements establish essentially identical relative values at 25 and 45 °C, R_1^{Val}/R_1^{Ile} = 2.0 ± 0.1. In fact, as we show below, both the ^{1}H and ^{13}C line widths for I159δ1 and I161δ1 are significantly larger than for V169γ at 50 °C, with the differences becoming pronounced already at 30 °C.

By means of comparison we have also recorded ^{13}C detected FROSTY-MAS[33]-based HETCOR spectra where the ^{1}H-to-^{13}C polarization transfer step is carried out using an INEPT scheme[52] (MAS INEPT HETCOR, Figure 1B-ii). The INEPT transfer will preferentially "select" flexible regions so that the solid-state data set recorded in this manner is very similar to the solution spectrum, with intense correlations observed for I159δ1, I161δ1, and Val169γ methyl groups. All correlations increase significantly with temperature from −22 to 0 °C. Interestingly, both Ile peaks decrease in intensity from 0 to 30 °C, consistent with an exchange process, as observed in the solution state, although in solution the increased line broadening from exchange is compensated to some extent by more rapid overall tumbling as the temperature increases. FROSTY-MAS HETCOR spectra have also been obtained with ^{1}H-to-^{13}C cross-polarization[48,51] (MAS FSLG-CP HETCOR, Figure 1B-iii) that are very similar to those previously recorded by Reif and co-workers.[33] Notably, at −22 °C a resonance from I159δ1 is observed at 9.5 ppm, in contrast to 12.3 ppm for the corresponding peak in the solution state or in FROSTY spectra recorded with INEPT magnetization transfer. Cross peaks are observed between I159δ1 and I133δ1,V93γ methyl groups in 2D ^{13}C−^{13}C RFDR spectra[49] (Figure S2), consistent with X-ray structures of a number of sHSPs[27−29] and with a recent solid-state NMR-derived model of the αB-crystallin core dimer[10] where the IxI motif is rigidly attached to an adjacent dimer in the structure. The FROSTY-MAS spectra presented here thus provide strong evidence for the IxI moiety populating two conformations at low temperature (−22 °C), one that is tightly bound and a second that is disordered and very similar to the major conformation in solution, that is the dominant form at higher temperatures.

In order to probe the conformational exchange process involving the Ile residues (see above) in more detail and to understand how the inter-converting states may be related structurally, we have carried out solution-state CPMG[53,54] RD experiments (Figure 2). The single-quantum ^{13}C RD profiles[42] obtained for both I159δ1 and I161δ1 show the characteristic signature of exchange with effective transverse relaxation rates, $R_{2,eff}$, decreasing as a function of increasing pulse rate (ν_{CPMG}). In contrast, the RD curves for the two methyl resonances from V169 are independent of ν_{CPMG}, consistent with the absence of chemical exchange or with a scenario where there is little chemical shift difference between exchanging states. A detailed analysis of the RD data presented previously[9] indicates that the major conformation, corresponding to the dynamic unbound IxI state, exchanges with a second conformer which has a maximum fractional population of 2% at 50 °C, pH 7,

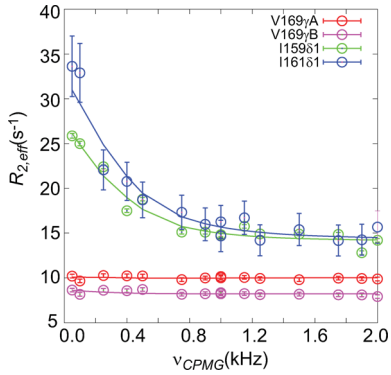

Figure 2. Relaxation dispersion NMR spectroscopy reveals millisecond time scale dynamics in the C-terminus of αB-crystallin. (A) Single-quantum ^{13}C RD curves of the four C-terminal methyl resonances,[42] I159δ1, I161δ1, V169γ1/γ2, pH 4.7, 50 °C, 18.8 T. RD curves of V169γ1/γ2 do not show evidence of exchange on the millisecond time scale. In contrast, the corresponding curves for I159δ1 and I161δ1 reveal a strong contribution from the effects of millisecond dynamics. Analysis of the data using a two-state exchange model, as described previously,[9] reveals an additional sparsely populated conformational state with a fractional population of 3% and lifetimes for the ground and excited states of 38 and 1 ms, respectively.[9] The sparsely populated state has been shown to regulate the subunit exchange process.[9] Methyl groups for V169 have not been stereospecifically assigned and hence are denoted "A" and "B".

increasing with decreasing pH.[9] The effects of exchange as a function of both pH and temperature as quantified by both NMR and mass spectrometry have been described previously,[8,9] establishing that the same exchange process manifests over the complete pH and temperature range examined. For completeness here, Figure S3 shows ^{1}H 1D, ^{13}C-edited NMR spectra recorded at a number of temperatures and pH values, with exchange contributions increasing at the lower pH values and at higher temperatures. As described in Materials and Methods and below, we have carried out further detailed RD experiments at pH 5 to maximize the observed exchange effects.

At the time of our initial relaxation experiments,[9] we were not able to determine the Ile ^{13}Cδ1 chemical shifts in the sparsely populated state since only the absolute values of the differences in shifts between exchanging conformers are available from RD data sets. The structural features of the IxI motif in the bound conformation were thus not established. Additionally, no information was available concerning the motional properties of IxI in the excited state. This information is critical to our model of subunit exchange that is described below.

With the recent development of $R_{1\rho}$ experiments that provide signs of chemical shift differences between exchanging states even in cases where large differences in intrinsic relaxation rates are present[55] (see below), we can now establish that the ^{13}C chemical shifts of I159δ1 and I161δ1 in the excited state are 10.5 and 14.1 ppm, respectively. These shifts are similar to those for the bound state from solid-state NMR at −22 °C (9.5 and 15 ppm respectively, Figure 1B-iii), indicating that the sparsely populated state may resemble the bound conformer observed by solid-state NMR.[10]

As described above, previous solution NMR studies have established that the IxI ground state is highly dynamic.[9] Further evidence is derived from the relative intensities of the ^{13}C methyl multiplet components recorded in an F_1-coupled HSQC data set. In such a spectrum four individual components

dx.doi.org/10.1021/ja307874r | J. Am. Chem. Soc. 2012, 134, 15343−15350

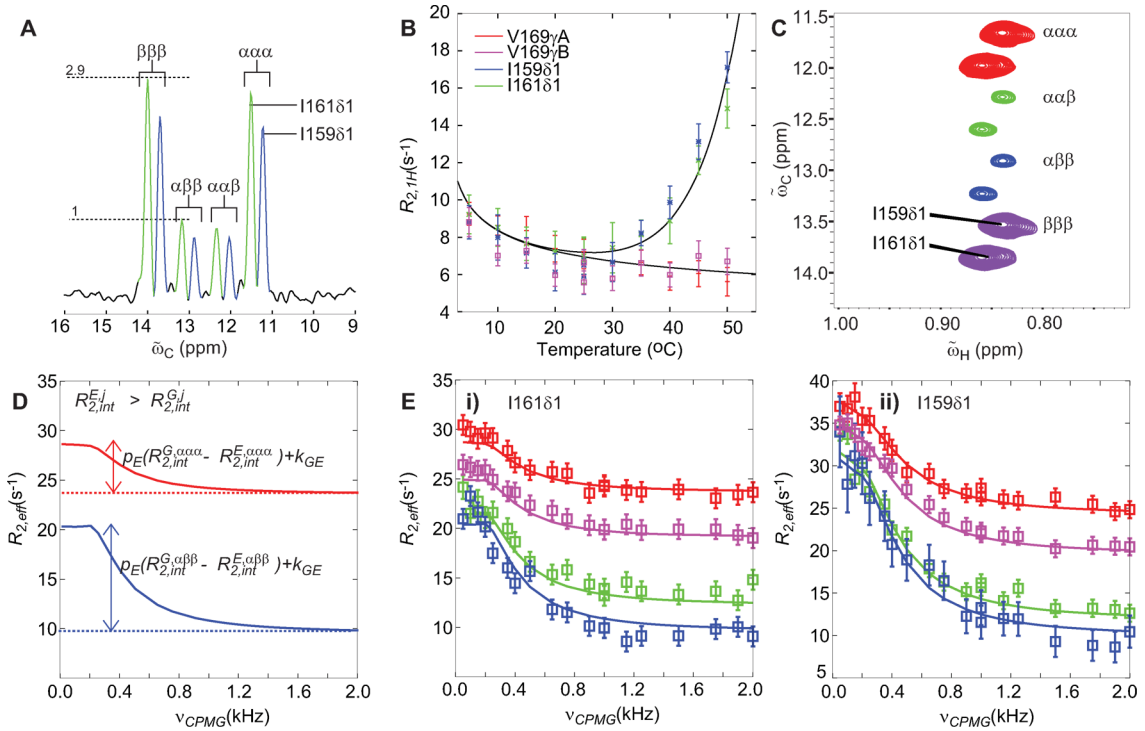

Figure 3. (A) Trace through a $^{1}H-^{13}C$ HSQC spectrum of U-[^{2}H], Ile-[$^{13}CH_3$ $\delta1$], Leu,Val-[$^{13}CH_3$,$^{12}CD_3$] αB-crystallin, 45 °C, 14.0T, pH 5, recorded without proton decoupling during acquisition of carbon chemical shift. The resonances from I159δ1 and I161δ1 are approximately in the ratio 3:1:1:3. (B) ^{1}H R_2 rates as a function of temperature for I159δ1, I161δ1, and V169γ1/γ2 (stereospecific assignments of V169 methyl groups are not available; hence V169 methyls are denoted "A" and "B"). Rates are measured as described previously.[9] $R_{2,1H}$ values for V169 decrease in a manner consistent with decreasing solution viscosity. Similarly, $R_{2,1H}$ rates for I159δ1 and I161δ1 decrease with increasing temperature in the range 0–20 °C, while at higher temperatures the rates increase rapidly. Solid lines in the figure are meant to guide the eye. (C) 2D $^{13}C-^{1}H$ correlation map, corresponding to the first plane of a spin-state-selective CPMG RD experiment,[45,57] with the four spin-state-selective multiplet components observed. The ^{1}H spin states associated with each multiplet line are as indicated with α and β, corresponding to ^{1}H spin up and down. (D) Fits of RD curves of the four separated ^{13}C methyl multiplet components can establish the dynamic properties of the sparsely populated ("invisible") state, as described in detail previously[45] and summarized in the text. A schematic illustrates that the sizes of the dispersion profiles (arrows) for the outer lines (only the most upfield line is shown) are smaller than for the inner lines (only one of the two is indicated) in the case where the methyl probe in the excited state is less dynamic than in the ground conformation. (E) RD curves of the four separated components for I159δ1 (i) and I161δ1 (ii) pH 5, 40°C, 18.8 T, analyzed and fit (solid lines) as described previously.[45] The sizes of dispersion profiles derived from the inner lines are larger than those from the outer lines for both residues, corresponding to $R_{2,int}^{E,j} > R_{2,int}^{G,j}$. Data were recorded at pH 5, where the population of the excited state, and so the magnitude of the difference in relaxation between the outer and inner lines, is maximal.

of the $^{13}CH_3$ group are observed corresponding to the ^{13}C spin coupled to protons either all "up" ($\alpha\alpha\alpha$) or "down" ($\beta\beta\beta$), outer multiplet components, or to protons in the "2-up/1-down" ($\alpha\alpha\beta$) or "2-down/1-up" ($\beta\beta\alpha$) states, inner components. For a highly dynamic methyl group there is little difference in transverse relaxation rates of each of the carbon lines, so a 3:1:1:3 multiplet structure is predicted.[32] In contrast, in the slow tumbling limit the net $^{13}C-^{1}H$ dipolar interaction is 3-fold larger for the outer lines, leading to a decay rate that is approximately 9 times more rapid than for the inner components.[56] Similar ratios of outer to inner components, 3.1:1 to 2.9:1, are found for both I159δ1 and I161δ1, confirming the highly dynamic nature of these residues in the ground state (Figure 3A). To obtain insight into the motional properties of these isoleucines in the excited state, we recorded the decay of methyl ^{1}H transverse magnetization,[41] $R_{2,1H}$, as a function of temperature (Figure 3B). As a control we also measured $R_{2,1H}$ values for the methyl protons of V169. These were found to decrease with temperature, as expected on the basis of decreasing solution viscosity and enhanced molecular tumbling. Between 0 and 20 °C, proton relaxation rates for I159δ1 and I161δ1 methyl groups also followed this trend. Above 20 °C, however, $R_{2,1H}$ values were found to increase significantly, and at 50 °C, ^{1}H transverse relaxation rates for the δ methyls of I159/I161 were approximately 3-fold larger than for the protons from methyls of V169. The increase in relaxation rates (minimum in R_2 vs temperature profile, Figure 3B) coincides precisely with the point at which the effects of chemical exchange become observable via ^{13}C CPMG RD. Moreover, ^{1}H CPMG RD profiles showed essentially no dependence on ν_{CPMG} over the complete temperature range (Figure S4). The simplest interpretation of the Ile relaxation data is, therefore, that the ^{1}H R_2 rate can be described in terms of a population-weighted average of ground- and excited-state relaxation rates, with the population of the excited state increasing with temperature and with R_2 values in the excited conformer greatly exceeding those in the ground state.

More quantitative information can be obtained by recording spin-state-selective ^{13}C methyl RD profiles, where each of the four lines of the multiplet component (Figure 3C) gives rise to a separate dispersion profile.[45] In the absence of relaxation differences between ground and excited states, the dispersion profiles for each of the four lines differ only by a vertical displacement. In contrast, when the relaxation rates for the ^{13}C methyl spin in question are different in each of the interconverting states, distinct profiles are observed that cannot be

dx.doi.org/10.1021/ja307874r | J. Am. Chem. Soc. 2012, 134, 15343–15350

superimposed, as illustrated schematically in Figure 3D.[45] The main features in this figure can be understood most simply by considering a two-state exchanging spin system in moderately slow exchange. In the limit that the CPMG pulsing rate is very slow, $\nu_{CPMG} \rightarrow 0$, $R_{2,eff}$ rates for each of the four lines are given by $R_{2,eff}^{G,j}(0) = k_{GE} + R_{2,int}^{G,j}$, $j \in \{\alpha\alpha\alpha,\alpha\alpha\beta,\alpha\beta\beta,\beta\beta\beta\}$, where $R_{2,int}^{G,j}$ is the intrinsic ^{13}C methyl j spin-state transverse relaxation rate for the ground-state conformer and k_{mn} is the rate of exchange from state m to n. In the case where pulsing is rapid, $\nu_{CPMG} \rightarrow \infty$, the value of $R_{2,eff}$ becomes the population-weighted average of relaxation rates in each of the inter-converting states (assuming that exchange is faster than $|R_{2,int}^{G} - R_{2,int}^{E}|$), $R_{2,eff}^{G,j}(\infty) = p_G R_{2,int}^{G,j} + p_E R_{2,int}^{E,j}$, where p_G and $p_E = 1 - p_G$ are the fractional populations of the ground and excited states, respectively. The "size" of the dispersion profile (arrow in Figure 3D) is thus given by $R_{2,eff}^{G,j}(0) - R_{2,eff}^{G,j}(\infty) = k_{GE} + p_E(R_{2,int}^{G,j} - R_{2,int}^{E,j})$. Noting that in the macromolecule limit (such as for proteins) the outer multiplet components relax more rapidly than the inner lines, $R_{2,int}^{\alpha\alpha\alpha}, R_{2,int}^{\beta\beta\beta} > R_{2,int}^{\alpha\alpha\beta}, R_{2,int}^{\alpha\beta\beta}$[45,56] (see above) and assuming that $R_{2,int}^{E,j} > R_{2,int}^{G,j}$, the schematic shown in Figure 3D is obtained where dispersion profiles from the inner lines are larger than those from the outer components. In contrast, when $R_{2,int}^{E,j} < R_{2,int}^{G,j}$, the situation is reversed. Figure 3E-i,ii shows RD profiles for each of the four lines for I159δ1 (i) and I161δ1 (ii) (18.8 T, 50 °C), and it is clear that substantial differences in the curves are obtained, exactly as predicted in Figure 3D. Even without a detailed analysis of the data, it follows simply by inspection that the excited-state conformation is one in which the Ile residues are very much less mobile than in the populated ground state. Fits (solid lines) to the experimental data (squares), measured at fields of 11.7, 14.0, and 18.8 T, using a two-site model of exchange were performed as described in detail previously,[45] assuming that both Ile residues report on the same exchange process (same populations and rates). An important parameter obtained from the fit is $\Delta(S^2\tau_c) = (S^2\tau_c)_E - (S^2\tau_c)_G$, where S^2 is a methyl axis order parameter and τ_c is the (assumed isotropic) correlation time in either the excited (E) or the ground (G) state. Values of $\Delta(S^2\tau_c) = +180$ and $+100$ ns were obtained for I159δ1 and I161δ1, respectively, confirming that the excited state is indeed bound.

The formation of the excited state has previously been linked with the process of subunit exchange in αB-crystallin.[9] The finding that it is bound leads to a straightforward model that can explain how subunit exchange occurs in terms of the formation and breaking of specific interactions within oligomers. Our previous studies have established that monomers of αB-crystallin (half-ellipses in Figure 4) are held in place within a given oligomer by two types of interactions.[8] The first is intra-dimer, depicted in our model in Figure 4 by a red ring, while the second class is inter-dimer, denoted by wavy lines (black or gray). A model that assumes only these two classes of interactions, which are essentially independent of oligomer size, quantitatively accounts for the oligomeric distributions observed over a wide range of solution conditions, as measured by mass spectrometry.[8] While the structural basis of the intra-dimer interactions is well understood,[10,25−27] the atomic contacts that constitute the inter-dimer interface are presently less well known. Previous work using NMR paramagnetic relaxation enhancement measurements has shown that the intrinsically disordered "ground state" of the C-terminus (yellow) makes transient contacts with a specific hydrophobic groove on adjacent monomers,[9] contributing to the stabilization of the inter-dimer interface (denoted by gray wavy lines in Figure 4). Other interactions between monomers or involving the N-terminus have also been identified as contributing toward the stability of this interface[27] and are denoted by black wavy lines.

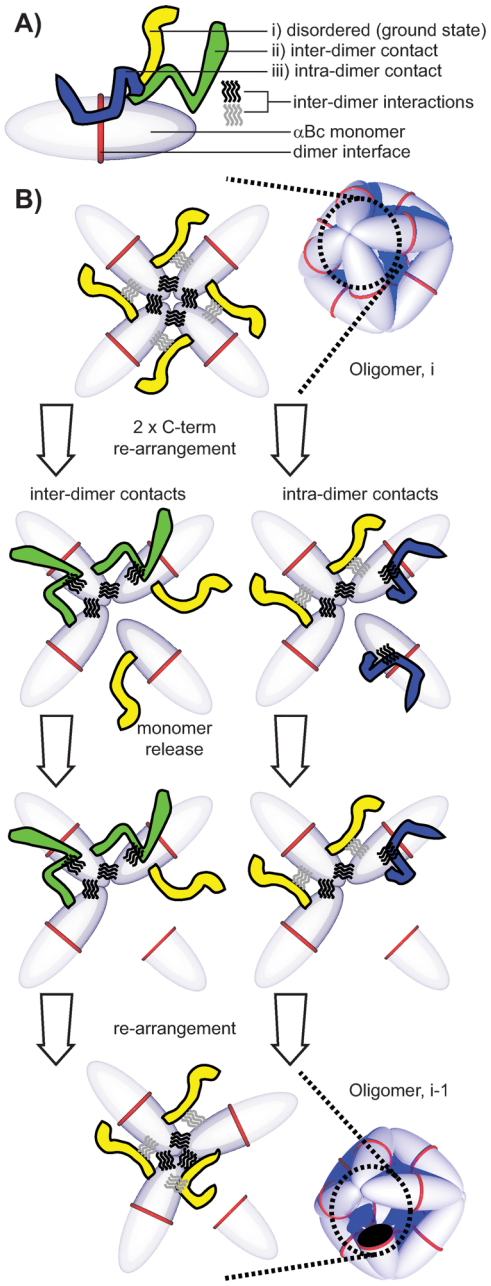

Figure 4. Microscopic mechanism for monomer dissociation and subunit exchange of αB-crystallin oligomers. Although the model is illustrated for an octahedral 24-mer ("oligomer i") it applies equally to any polyhedral structure where an integer number of monomers come together about a vertex. Details are given in the text.

Using results from a combination of mass spectrometry,[8] X-ray diffraction,[25] and NMR[9] analyses, we concluded previously[11] that (1) all monomers must be in equivalent environments, (2) oligomers are comprised of dimeric building blocks, (3) each monomer is connected to an oligomer via a pair of C-terminal "cross-linking" interactions that must be broken prior to monomer release, and (4) models of oligomers could be constructed based on polyhedral scaffolds. Taken together, in concert with experimental data from ion-mobility

dx.doi.org/10.1021/ja307874r | J. Am. Chem. Soc. 2012, 134, 15343−15350

mass spectrometry and electron microscopy,[11] the structure of a 24-mer can be described by an octahedron, shown schematically in Figure 4B ("oligomer i"). Focusing on a single polyhedral vertex (they are all the same), it is clear that four dimers come together with each specific monomer interacting with its two immediate neighbors (black and gray wavy lines). In order for a monomer to dissociate from the oligomer, therefore, both of the "immediate neighbor" stabilizing interactions must be broken. Supporting this notion, NMR RD and mass spectrometry kinetic data[9] can be reconciled assuming that the dissociation process involves the simultaneous rearrangement of a pair of C-termini (including IxI motifs), as depicted in the model described by Figure 4. Here, disordered C-termini, corresponding to ground states (yellow), simultaneously form ordered low-populated conformers, denoted here as either inter-dimer (green, left side) or intra-dimer (blue, right side), leading to the release of the C-terminal interactions. In this model, formation of either two inter- or two intra-dimer C-terminal interactions, or a mixture of both, corresponding to an ordering of the IxI region, results in a distortion of the oligomer, leading to the breaking of interactions that hold a specific monomer in place and thereby facilitating its departure. Subsequently the structure rearranges so that all monomers occupy an identical environment. The model thus provides a link between the macroscopic process of subunit exchange and microscopic fluctuations of the C-terminal IxI.

CONCLUDING REMARKS

The present study establishes that at least two distinct structural environments are adopted by the C-terminal IxI residues of αB-crystallin, one free and one bound, with relative populations varying substantially with temperature. While both disordered and bound states are seen at low temperatures, above 0 °C only the highly mobile conformation is appreciably populated. Interestingly, this "ground"-state conformer exchanges with a second sparsely populated state where the IxI moiety is much more rigid ("bound") and where the ^{13}C Ile δ1 methyl chemical shifts are similar to those reported from a solid-state NMR study of αB-crystallin at low temperature.[10] The excited state has been shown previously to play an important role in controlling the kinetics and thermodynamics of subunit interchange between different oligomers and the resulting particle size distribution.[8,9] Intriguingly, the present study has established that the excited-state conformation of the IxI motif shares several important features with the "bound"-state structure reported from both solid-state NMR and X-ray methods,[10,27] leading to a proposed mechanism for the subunit exchange process. The complementary information derived here from both solid- and solution-state NMR experiments is important for elucidating the detailed mechanism by which dynamics are able to regulate the function of this important molecule.

ASSOCIATED CONTENT

Supporting Information

Figures showing assignment of I159/161 δ1 methyl groups, solid-state NMR spectra, effects of pH and temperature on I159/161 and V169 ^{1}H NMR spectra, and ^{1}H/^{13}C CPMG RD profiles of αB-crystallin. This material is available free of charge via the Internet at http://pubs.acs.org.

AUTHOR INFORMATION

Corresponding Author

kay@pound.med.utoronto.ca; ajb204@gmail.com

Present Address

[‖]Institute of Structural and Molecular Biology, University College London, London WC1E 6BT, U.K.

Notes

The authors declare no competing financial interest.

ACKNOWLEDGMENTS

A.J.B. acknowledges funding in the form of a Canadian Institutes of Health Research (CIHR) postdoctoral fellowship. This work was supported by a grant from the Natural Sciences and Engineering Research Council of Canada (L.E.K.). P.W. is funded by a Canada Graduate Scholarship from CIHR, J.L.P.B. is a Royal Society University Research Fellow, G.R.H. acknowledges funding from the Wellcome Trust, S.S. holds a Canada Research Chair in structural biology, and L.E.K. holds a Canada Research Chair in biochemistry. The authors are grateful to Prof. B. Reif, Munich, and Dr. A. Mainz for making available a FROSTY-MAS HETCOR spectrum of αB-crystallin.

REFERENCES

(1) Baldwin, A. J.; Knowles, T. P.; Tartaglia, G. G.; Fitzpatrick, A. W.; Devlin, G. L.; Shammas, S. L.; Waudby, C. A.; Mossuto, M. F.; Meehan, S.; Gras, S. L.; Christodoulou, J.; Anthony-Cahill, S. J.; Barker, P. D.; Vendruscolo, M.; Dobson, C. M. *J. Am. Chem. Soc.* **2011**, *133*, 14160−14163.

(2) Hartl, F. U.; Bracher, A.; Hayer-Hartl, M. *Nature* **2011**, *475*, 324−332.

(3) Haslbeck, M.; Franzmann, T.; Weinfurtner, D.; Buchner, J. *Nat. Struct. Mol. Biol.* **2005**, *12*, 842−846.

(4) Balch, W. E.; Morimoto, R. I.; Dillin, A.; Kelly, J. W. *Science (New York)* **2008**, *319*, 916−919.

(5) Richter, K.; Haslbeck, M.; Buchner, J. *Mol. Cell* **2010**, *40*, 253−266.

(6) Ecroyd, H.; Carver, J. A. *Cell. Mol. Life Sci.* **2009**, *66*, 62−81.

(7) Shinohara, H.; Inaguma, Y.; Goto, S.; Inagaki, T.; Kato, K. *J Neurol Sci* **1993**, *119*, 203−208.

(8) Baldwin, A. J.; Lioe, H.; Robinson, C. V.; Kay, L. E.; Benesch, J. L. *J. Mol. Biol.* **2011**, *413*, 297−309.

(9) Baldwin, A. J.; Hilton, G. R.; Lioe, H.; Bagneris, C.; Benesch, J. L.; Kay, L. E. *J. Mol. Biol.* **2011**, *413*, 310−320.

(10) Jehle, S.; Rajagopal, P.; Bardiaux, B.; Markovic, S.; Kuhne, R.; Stout, J. R.; Higman, V. A.; Klevit, R. E.; van Rossum, B. J.; Oschkinat, H. *Nat. Struct. Mol. Biol.* **2010**, *17*, 1037−1042.

(11) Baldwin, A. J.; Lioe, H.; Hilton, G. R.; Baker, L. A.; Rubinstein, J. L.; Kay, L. E.; Benesch, J. L. *Structure* **2011**, *19*, 1855−1863.

(12) Braun, N.; Zacharias, M.; Peschek, J.; Kastenmuller, A.; Zou, J.; Hanzlik, M.; Haslbeck, M.; Rappsilber, J.; Buchner, J.; Weinkauf, S. *Proc. Natl. Acad. Sci. U.S.A.* **2011**, *108*, 20491−20496.

(13) Jehle, S.; Vollmar, B. S.; Bardiaux, B.; Dove, K. K.; Rajagopal, P.; Gonen, T.; Oschkinat, H.; Klevit, R. E. *Proc. Natl. Acad. Sci. U.S.A.* **2011**, *108*, 6409−6414.

(14) Basha, E.; O'Neill, H.; Vierling, E. *Trends Biochem. Sci.* **2011**, *37*, 106−117.

(15) Clark, A. R.; Lubsen, N. H.; Slingsby, C. *Int. J. Biochem. Cell Biol.* **2012**, *44*, 1687−1697.

(16) Hilton, G. R.; Lioe, H.; Stengel, F.; Baldwin, A. J.; Benesch, J. L. *Top. Curr. Chem.: Molecular Chaperones* **2012**, DOI: 10.1007/128_2012_324.

(17) Carver, J. A.; Aquilina, J. A.; Truscott, R. J.; Ralston, G. B. *FEBS Lett.* **1992**, *311*, 143−149.

(18) Ghahghaei, A.; Rekas, A.; Carver, J. A.; Augusteyn, R. C. *Mol. Vis.* **2009**, *15*, 2411−2420.

(19) Treweek, T. M.; Rekas, A.; Walker, M. J.; Carver, J. A. *Exp. Eye Res.* **2010**, *91*, 691−699.
(20) Pasta, S. Y.; Raman, B.; Ramakrishna, T.; Rao, Ch, M. *Mol. Vis.* **2004**, *10*, 655−662.
(21) Hayes, V. H.; Devlin, G.; Quinlan, R. A. *J. Biol. Chem.* **2008**, *283*, 10500−10512.
(22) Inagaki, N.; Hayashi, T.; Arimura, T.; Koga, Y.; Takahashi, M.; Shibata, H.; Teraoka, K.; Chikamori, T.; Yamashina, A.; Kimura, A. *Biochem. Biophys. Res. Commun.* **2006**, *342*, 379−386.
(23) Pilotto, A.; Marziliano, N.; Pasotti, M.; Grasso, M.; Costante, A. M.; Arbustini, E. *Biochem. Biophys. Res. Commun.* **2006**, *346*, 1115−1117.
(24) Devi, R. R.; Yao, W.; Vijayalakshmi, P.; Sergeev, Y. V.; Sundaresan, P.; Hejtmancik, J. F. *Mol. Vis.* **2008**, *14*, 1157−1170.
(25) Bagneris, C.; Bateman, O. A.; Naylor, C. E.; Cronin, N.; Boelens, W. C.; Keep, N. H.; Slingsby, C. *J. Mol. Biol.* **2009**, *392*, 1242−1252.
(26) Clark, A. R.; Naylor, C. E.; Bagneris, C.; Keep, N. H.; Slingsby, C. *J. Mol. Biol.* **2011**, *408*, 118−134.
(27) Laganowsky, A.; Benesch, J. L.; Landau, M.; Ding, L.; Sawaya, M. R.; Cascio, D.; Huang, Q.; Robinson, C. V.; Horwitz, J.; Eisenberg, D. *Protein Sci.* **2010**, *19*, 1031−1043.
(28) Kim, K. K.; Kim, R.; Kim, S. H. *Nature* **1998**, *394*, 595−599.
(29) van Montfort, R. L.; Basha, E.; Friedrich, K. L.; Slingsby, C.; Vierling, E. *Nat. Struct. Biol.* **2001**, *8*, 1025−1030.
(30) Hansen, D. F.; Neudecker, P.; Kay, L. E. *J. Am. Chem. Soc.* **2010**, *132*, 7589−7591.
(31) Sprangers, R.; Kay, L. E. *Nature* **2007**, *445*, 618−622.
(32) Tugarinov, V.; Hwang, P. M.; Ollerenshaw, J. E.; Kay, L. E. *J. Am. Chem. Soc.* **2003**, *125*, 10420−10428.
(33) Mainz, A.; Jehle, S.; van Rossum, B. J.; Oschkinat, H.; Reif, B. *J. Am. Chem. Soc.* **2009**, *131*, 15968−15969.
(34) Bertini, I.; Luchinat, C.; Parigi, G.; Ravera, E.; Reif, B.; Turano, P. *Proc. Natl. Acad. Sci. U.S.A.* **2011**, *108*, 10396−10399.
(35) Meehan, S.; Knowles, T. P.; Baldwin, A. J.; Smith, J. F.; Squires, A. M.; Clements, P.; Treweek, T. M.; Ecroyd, H.; Tartaglia, G. G.; Vendruscolo, M.; Macphee, C. E.; Dobson, C. M.; Carver, J. A. *J. Mol. Biol.* **2007**, *372*, 470−484.
(36) Ruschak, A. M.; Kay, L. E. *J. Biomol. NMR* **2010**, *46*, 75−87.
(37) Sprangers, R.; Velyvis, A.; Kay, L. E. *Nat. Methods* **2007**, *4*, 697−703.
(38) Tugarinov, V.; Sprangers, R.; Kay, L. E. *J. Am. Chem. Soc.* **2007**, *129*, 1743−1750.
(39) Ollerenshaw, J. E.; Tugarinov, V.; Kay, L. E. *Magn. Reson. Chem.* **2003**, *41*, 843−852.
(40) Delaglio, F.; Grzesiek, S.; Vuister, G. W.; Zhu, G.; Pfeifer, J.; Bax, A. *J. Biol. NMR* **1995**, *V6*, 277−293.
(41) Tugarinov, V.; Kay, L. E. *J. Am. Chem. Soc.* **2006**, *128*, 7299−7308.
(42) Lundstrom, P.; Vallurupalli, P.; Religa, T. L.; Dahlquist, F. W.; Kay, L. E. *J. Biomol. NMR* **2007**, *38*, 79−88.
(43) Hansen, D. F.; Vallurupalli, P.; Lundstrom, P.; Neudecker, P.; Kay, L. E. *J. Am. Chem. Soc.* **2008**, *130*, 2667−2675.
(44) Vallurupalli, P.; Hansen, D. F.; Stollar, E.; Meirovitch, E.; Kay, L. E. *Proc. Natl. Acad. Sci. U.S.A.* **2007**, *104*, 18473−18477.
(45) Hansen, D. F.; Vallurupalli, P.; Kay, L. E. *J. Am. Chem. Soc.* **2009**, *131*, 12745−12754.
(46) Bennett, A. E.; Rienstra, C. M.; Auger, M.; Lakshmi, K. V.; Griffin, R. G. *J. Chem. Phys.* **1995**, *103*, 6951−6958.
(47) Bielecki, A.; Burum, D. P. *J. Magn. Reson., Ser. A* **1995**, *116*, 215−220.
(48) Metz, G.; Wu, X. L.; Smith, S. O. *J. Magn. Reson., Ser. A* **1994**, *110*, 219−227.
(49) Ishii, Y. *J. Chem. Phys.* **2001**, *114*, 8473−8483.
(50) Bielecki, A.; Kolbert, A. C.; Levitt, M. H. *Chem. Phys. Lett.* **1989**, *155*, 341−346.
(51) van Rossum, B. J.; Farster, H.; de Groot, H. J. M. *J. Magn. Reson.* **1997**, *124*, 516−519.
(52) Morris, G. A.; Freeman, R. *J. Am. Chem. Soc.* **1979**, *101*, 760−762.
(53) Meiboom, S.; Gill, D. *Rev. Sci. Instrum.* **1958**, *29*, 688−691.
(54) Carr, H. Y.; Purcell, E. M. *Phys. Rev. J1−PR* **1954**, *94*, 630−638.
(55) Baldwin, A. J.; Kay, L. E. *J Biomol NMR* **2012**, *53*, 1−12.
(56) Kay, L. E.; Torchia, D. A. *J. Magn. Reson.* **1991**, *95*, 536−547.
(57) Baldwin, A. J.; Hansen, D. F.; Vallurupalli, P.; Kay, L. E. *J. Am. Chem. Soc.* **2009**, *131*, 11939−11948.